

EUROPEAN ORGANIZATION FOR NUCLEAR RESEARCH
Proposal to the ISOLDE and Neutron Time-of-Flight Committee

Measurement of $^{40}\text{K}(n,p)$ and $^{40}\text{K}(n,\alpha)$ cross sections at n_TOF
EAR-2

September 27, 2022

Claudia Lederer-Woods¹, Moshe Friedman², Umberto Battino³, Ulli Koester⁴, Emilio Maugeri⁵, Michael Bacak⁶, Alberto Mengoni⁶, Thomas E. Cocolios⁷, Sergio Cristallo^{8,9}, Thomas Davinson¹, Nikolay Sosnin¹, Philip J Woods¹, Jozef Andrzejewski¹⁰, Aleksandra Gawlik-Ramiega¹⁰, Jaroslaw Perkowski¹⁰, and the n_TOF Collaboration

¹ *School of Physics and Astronomy, University of Edinburgh, UK*

² *Racah Institute of Physics, The Hebrew University of Jerusalem, Israel*

³ *University of Hull, UK*

⁴ *ILL Grenoble, France*

⁵ *PSI Villigen, Switzerland*

⁶ *CERN, Switzerland*

⁷ *KU Leuven, Belgium*

⁸ *Istituto Nazionale di Fisica Nucleare, Sezione di Perugia, Italy*

⁹ *Istituto Nazionale di Astrofisica - Osservatorio Astronomico di Teramo, Italy*

¹⁰ *University of Lodz, Poland*

Spokesperson: Claudia Lederer-Woods [claudia.lederer@ed.ac.uk]

Moshe Friedman [moshe.friedman@mail.huji.ac.il]

Technical coordinator: Oliver Aberle [oliver.aberle@cern.ch]

Abstract: ^{40}K is one of the main isotopes responsible for radiogenic heating in earth-like exoplanets. Stellar models suggest that a significant contribution to ^{40}K in our cosmos comes from the slow neutron capture process in massive stars. Abundances produced in the s process are sensitive to the destruction cross sections $^{40}\text{K}(n,\alpha)$, $^{40}\text{K}(n,p)$ and $^{40}\text{K}(n,\gamma)$. There is just one direct measurement of $^{40}\text{K}(n,\alpha)$ and $^{40}\text{K}(n,p)$ reaction cross sections at stellar neutron energies, however these data do not cover the entire range of astrophysical interest. We propose to measure $^{40}\text{K}(n,p)$ and $^{40}\text{K}(n,\alpha)$ reaction cross section at n_TOF EAR-2.

Requested protons: 5×10^{18} protons on target

Experimental Area: EAR2



1 Introduction

^{40}K ($T_{1/2} = 1.25 \times 10^9$ y) is a primordial isotope naturally occurring on earth. ^{40}K is one of the main isotopes responsible for heat generation in earth-like planets, by energy released when it β -decays (so-called radiogenic heating), and has been found to dominate the heating in young exoplanets [1]. Radiogenic heating is essential to sustain the crustal recycling (e.g. plate tectonics), which is considered advantageous for long-term biosphere habitability. It also impacts on CO_2 outgassing rates, which need to be at the right level to sustain habitability (too small rates cause global surface glaciation, while too high rates a too hot climate) [2]. Hence, the initial quantity of ^{40}K in an exoplanet is an important parameter to determine its habitability.

^{40}K is produced in massive stars during oxygen burning when lighter elements fuse in the cores of massive stars and in the slow neutron capture process (s-process) [3]. In the s-process, it is produced by neutron capture reactions on stable ^{39}K . Besides radiative neutron capture, (n, α) and (n, p) reactions are considered the main destruction channels for ^{40}K , with (n, α) predicted to have the largest reaction rate at the relevant stellar temperatures of 0.4 and 1 GK [7]. Figures 1 and 2 show results from a multi-zone post processing calculation of s-process nucleosynthesis of a star with 25 solar masses, and sub-solar metallicity ($Z = 0.006$) in the mass region around $A = 40$. In general, isotopes in that mass region have small overproduction factors, except for ^{40}K and ^{40}Ar , which are efficiently produced. The Figures also show results for various changes in the stellar $^{40}\text{K}(n, \alpha)$ and $^{40}\text{K}(n, p)$ reaction rates, respectively, namely that a factor 2 higher $^{40}\text{K}(n, \alpha)$ rate reduces the ^{40}K abundance by about 30%, while a factor two higher $^{40}\text{K}(n, p)$ rate mainly impacts on the production of ^{40}Ar , causing a 30% increase.

The study of the $^{40}\text{K}(n, \alpha)^{37}\text{Cl}$ reaction is of interest for the evolution of low mass stars too. In particular, this reaction works during the s-process in Asymptotic Giant Branch Stars (AGBs), thus fixing the chlorine isotopic ratio in these stellar objects. Kahane et al [4] measured such a ratio in the circumstellar envelope of the star IRC+10216, demonstrating that the initial mass of this object is between 1.5 and 3.0 M_{\odot} . We aim at better constraining such a mass range by reducing the uncertainty affecting the $^{40}\text{K}(n, \alpha)^{37}\text{Cl}$ rate.

Data on $^{40}\text{K}(n, \alpha)$ and $^{40}\text{K}(n, p)$ are scarce, and in particular at energies relevant to the s-process there is only one direct measurement [5] which was performed at the Joint Research Centre Geel using a KCl target 80% enriched in ^{40}K . Protons and α -particles were detected with a silicon surface barrier detector and the different reaction channels could be separated due to the different energy signals in the detector. In this measurement, resonance kernels for (n, α) and (n, p) reactions separately could be determined up to 20 keV neutron energy, while the summed cross section is published up to 70 keV. In addition, there has recently been a measurement of the time-reverse process $^{40}\text{Ar}(p, n)$ [6], however stellar $^{40}\text{K}(n, p)$ reaction rates could only be provided above 0.4 GK stellar temperature, and uncertainties were 15%. We propose to perform a measurement of $^{40}\text{K}(n, \alpha)$ and $^{40}\text{K}(n, p)$ cross sections, taking advantage of the large neutron energy range and high neutron flux available at n_TOF EAR-2.

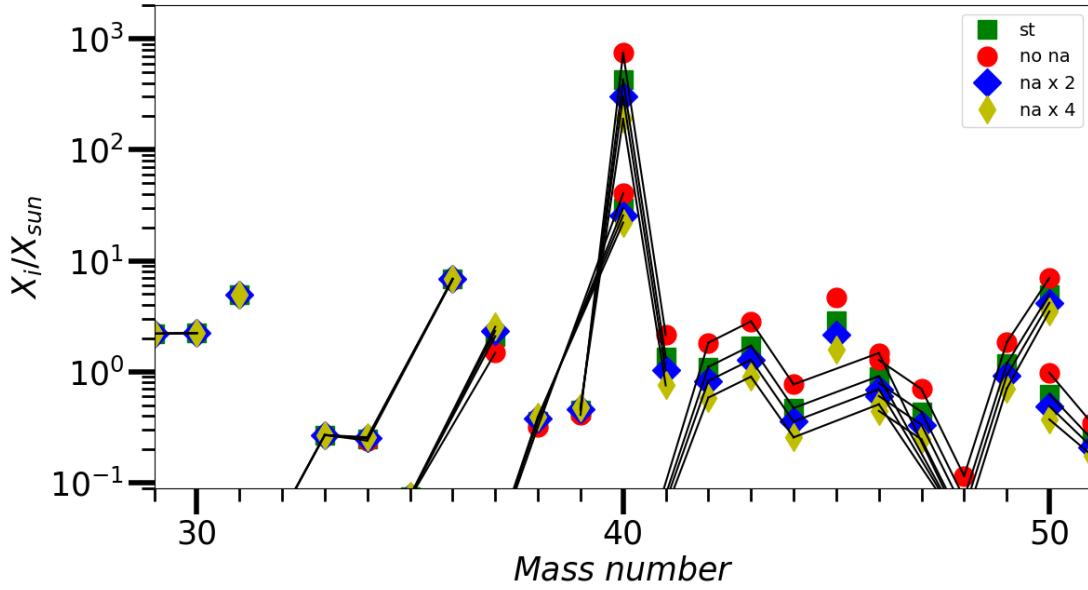


Figure 1: Overproduction factors after s-process nucleosynthesis in a massive star (25 solar masses, metallicity $Z = 0.006$), showing the impact on produced abundances around mass region $A = 40$ when changing the $^{40}\text{K}(n, \alpha)$ stellar rate. Green squares are standard rates, blue diamonds rate x 2, yellow diamonds rate x4, and red circles corresponds to a rate equal to zero. A change in the $^{40}\text{K}(n, \alpha)$ rate affects abundances from ^{37}Cl onwards.

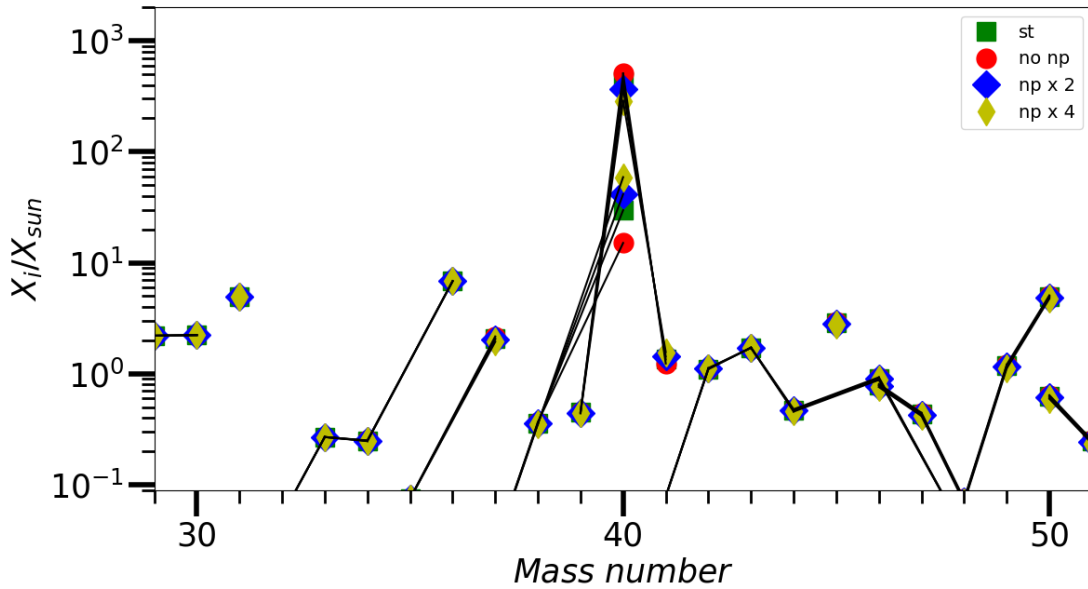


Figure 2: Same as Fig. 1, but for the stellar $^{40}\text{K}(n, p)$ rate.

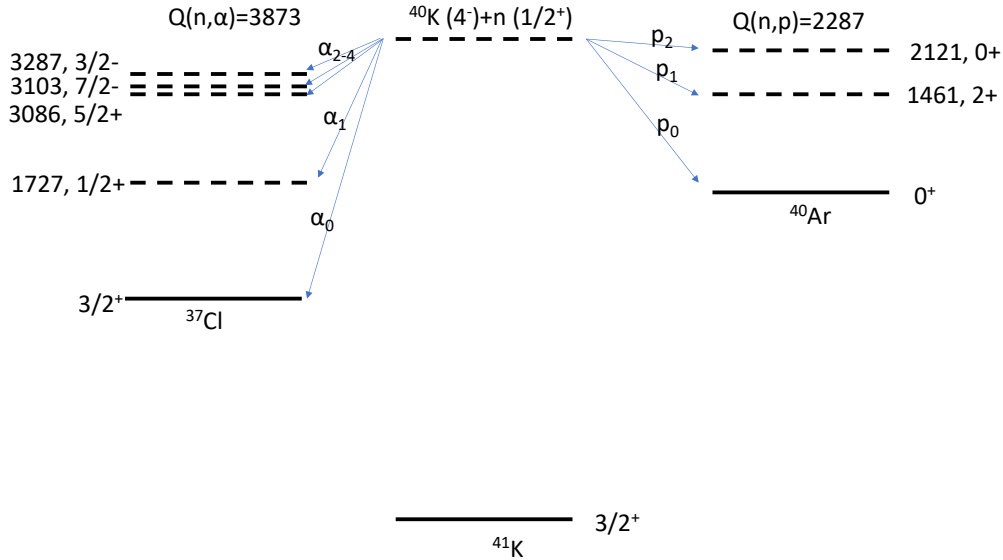


Figure 3: Scheme of the $^{40}\text{K}+n$ reaction with the possible α - and proton-decay channels. All energies are given in keV.

2 Method

A ^{40}K sample of $100\mu\text{g}$ and 80% isotopic enrichment will be produced at KU Leuven by implanting K on a thin carbon backing. If production of the samples using that technique fails, we will produce a KCl sample of lower enrichment (16%), by means of molecular plating, but again containing a total of $80\mu\text{g}$ ^{40}K . Both methods of production will result in good homogeneity, which will minimise effects of energy straggling from protons and alphas in the sample material. The $^{40}\text{K}(n, \alpha)$ reaction produces α -particles at energies of 3.5 MeV (producing ^{37}Cl in its ground state), and at energies of 1.8 MeV (producing ^{37}Cl in its first excited state). It is also energetically possible to populate higher lying states, however, the Coulomb barrier for these small α -energies of a few hundred keV suggest that the contribution of those channels is small. For the case of $^{40}\text{K}(n, p)^{40}\text{Ar}$, proton energies to the ground state are around 2.2 MeV, while they are only 0.8 MeV to the first excited state of ^{40}Ar . The $^{40}\text{K}(n, p)$ and $^{40}\text{K}(n, \alpha)$ reaction mechanisms are illustrated in Fig. 3.

Both reaction channels can be measured simultaneously taking advantage of the $dE - E$ technique, which we already used for the $^{26}\text{Al}(n, \alpha)$ and $^{26}\text{Al}(n, p)$ cross section measurement [8, 9]. The setup will consist of a thin silicon strip detector of $20\mu\text{m}$ thickness followed by a $300\mu\text{m}$ thick detector. Protons from the reaction into the ground state (n, p_0) will deposit around 500 keV energy in the $20\mu\text{m}$ dE -detector, and then be stopped in the $300\mu\text{m}$ E -detector, while α particles and (n, p_1) protons will be stopped in the dE -detector. This setup will provide an even better separation between protons and α 's than using only one silicon detector like in Ref. [5] and we expect to be able to separate proton and alpha channels also for the highest neutron energies measured.

The neutron beam will be monitored with a dedicated silicon detection setup SiMON-2 already installed. The data will be normalised by measuring relative to the reference reactions $^{10}\text{B}(n, \alpha)$ and $^6\text{Li}(n, t)$, using samples with the same diameter and a well known areal density.

3 Beam Time Estimate

The beam time was estimated based on the sample properties described above, and the simulated neutron flux and profile for a distance of 19.4 m from the spallation target, which corresponds to about 1 m from the floor of EAR-2. The simulated neutron flux is in good agreement with first measurements. The detection efficiency of the $dE - E$ system was estimated in Monte Carlo simulations. Furthermore, we adopt the cross section published by Weigmann et al. [5], which is a sum of the $^{40}\text{K}(n, \alpha) + ^{40}\text{K}(n, p)$ channels, since this is the only experimental data available in the keV region. To take into account the resolution at EAR-2, the Weigmann cross section is folded with the EAR-2 resolution function. It should be noted that this represents a worst case scenario of the resolution, since the Weigmann cross section provided to the databases is broadened from the finite experimental resolution at JRC Geel already, and the n_TOF resolution is expected to improve with the new spallation target (the resolution function was taken from the last phase with the old spallation target, but will be determined in a separate campaign for the new spallation target).

The left panel of Figure 4 shows the expected number of counts / bin for the sum of α +proton events for 4.5×10^{18} protons for the neutron energy range from thermal to 100 keV. The right panel shows a zoom into the tens of keV region, most relevant for s-process nucleosynthesis. At low energies, counting statistics are expected to be high, which will allow us to determine the thermal (25 meV) cross sections with high accuracy. From 10 keV onwards, it may become challenging to distinguish individual smaller resonances in the cross section due to resolution broadening effects. Table 1 lists the expected counts in a resonance for each channel separately, based on the information in Weigmann et al. This has been calculated using the unbroadened data. For the (n, α) channel, we expect more than 10 counts in most resonances, while the weaker (n, p) branch seems to be more challenging, but we will still be able to analyse several resonances. In addition, since we expect the (n, p) channel to be essentially background-free (due to taking advantage of coincident dE and E detection), we will be able to determine an accurate averaged cross section over the entire astrophysical neutron energy range. Irrespective of up to which neutron energy individual resonances can be resolved, the stellar rate can be calculated with high accuracy from the averaged cross section data for both channels. Since our setup will easily distinguish protons and α -particles, we will be able to determine the (n, α) and (n, p) cross section separately also above 20 keV, in contrast to Ref. [5]. Based on our previous measurement of $^{26}\text{Al}(n, \alpha)$ and $^{26}\text{Al}(n, p)$ reactions, we can at least measure the cross section up to 150 keV (likely higher). A count rate estimate of the high energy region, based on evaluated cross sections from the ENDF/B-VIII evaluation is shown in Fig. 5 which demonstrates that the cross section can be measured with good counting statistics also in the few hundred keV region. Therefore, we request 4.5×10^{18}

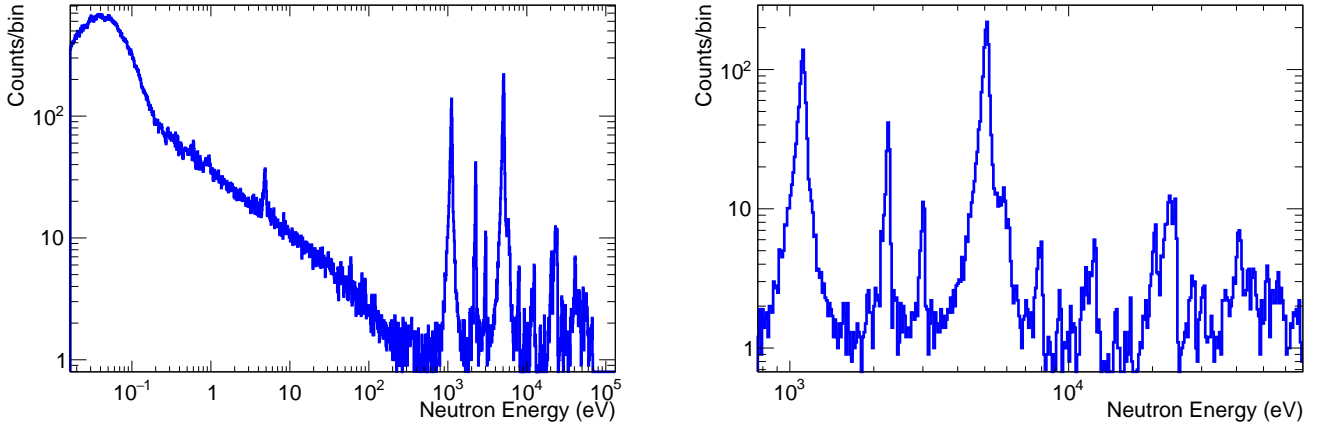


Figure 4: (Left) Number of counts in the dE-E system for the sum of $^{40}\text{K}(n, \alpha) + ^{40}\text{K}(n, p)$ reactions for 4.5×10^{18} protons. The data have been broadened to account for the facility resolution. (Right) Zoom in the higher energy region from about 1 to 100 keV.

protons for the measurement on ^{40}K . In addition, we request 0.5×10^{18} protons for measuring ^{10}B and ^6Li samples for normalising the data, and for performing background measurements without a sample in the reaction chamber.

E_R (keV)	(n, α) counts	(n, p) counts	E_R (keV)	(n, α) counts	(n, p) counts
1.128	1272	12	10.4	5	5
2.291	228	4	11.7	14	6
3.06	5	63	12.2	9	1
5.177	1864	18	12.7	37	4
5.98	17	53	15.3	10	2
6.21	47	5	17.0	7	0
7.87	16	1	19.3	14	1
8.1	31	0	20.9	41	4
9.42	6	9			

Table 1: Expected counts of α 's and protons for a resonance with neutron energy E_R . The calculation is based on data from Weigmann et al. [5]

Summary of requested protons: 5×10^{18} protons

References

- [1] E.A. Frank, B.S. Meyer, S.J. Mojzsis. *Icarus* **243**, 274-286 (2014).
- [2] B. J. Foley and A. J. Smye, *Astrobiology* **18**, 873 (2018).
- [3] M. Pignatari, F. Herwig, R. Hirschi, *et al.*, *Astroph. J. Suppl. S.* **225**, 24 (2016).

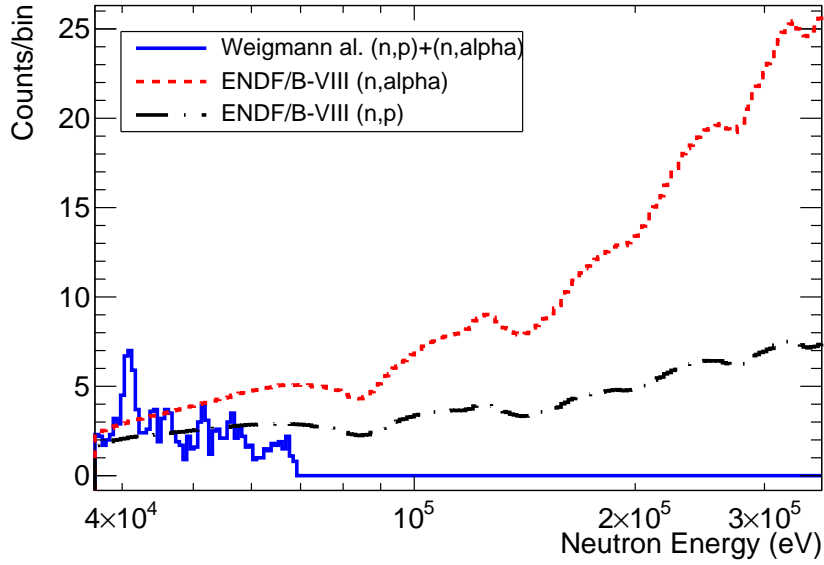


Figure 5: Number of counts in the dE-E system separately for proton and α channels at several hundred keV. The cross section was adopted from the ENDF/B-VIII evaluation. The low energy estimate based on Weigmann et al. is shown as well for comparison, indicating that the ENDF/B-VIII cross section may be over-estimated.

- [4] C. Kahane, *et al.*, AA **357**, 669 (2000).
- [5] H. Weigmann, C. Wagemans, A. Emsallem, M. Asghar, Nuclear Physics A **368**, 117-134 (1981).
- [6] P. Gastis, *et al.*, Physical Review C **101**, 055805 (2020).
- [7] T. Rauscher and F.-K. Thielemann, Atomic Data Nucl. Data Tables, 75, 1 (2000).
- [8] C. Lederer-Woods, *et al.* (n_TOF Collaboration), Physical Review C **104**, L022803 (2021).
- [9] C. Lederer-Woods, *et al.* (n_TOF Collaboration), Physical Review C **104**, L032803 (2021).

Appendix

DESCRIPTION OF THE PROPOSED EXPERIMENT

Please describe here below the main parts of your experimental set-up:

Part of the experiment	Design and manufacturing
If relevant, write here the name of the <u>fixed</u> installation you will be using [SiTe-EDI : Silicon Telescope setup used in P-406 (present at CERN)]	<input checked="" type="checkbox"/> To be used without any modification <input type="checkbox"/> To be modified
If relevant, write here the name of the <u>fixed</u> installation you will be using [SiMon-2]	<input checked="" type="checkbox"/> To be used without any modification <input type="checkbox"/> To be modified
If relevant, describe here the name of the <u>flexible/transported</u> equipment you will bring to CERN from your Institute [⁴⁰ K target: K of high (80%) enrichment implanted on a thin carbon backing]	<input type="checkbox"/> Standard equipment supplied by a manufacturer <input checked="" type="checkbox"/> CERN/collaboration responsible for the design and/or manufacturing
Small spare parts, such as detector holders, cabling, spare detectors etc.	<input checked="" type="checkbox"/> Standard equipment supplied by a manufacturer <input checked="" type="checkbox"/> CERN/collaboration responsible for the design and/or manufacturing
[insert lines if needed]	

HAZARDS GENERATED BY THE EXPERIMENT

Additional hazard from flexible or transported equipment to the CERN site:

Domain	Hazards/Hazardous Activities		Description
Mechanical Safety	Pressure	<input type="checkbox"/>	[pressure] [bar], [volume][l]
	Vacuum	<input type="checkbox"/>	
	Machine tools	<input type="checkbox"/>	
	Mechanical energy (moving parts)	<input type="checkbox"/>	
	Hot/Cold surfaces	<input type="checkbox"/>	
Cryogenic Safety	Cryogenic fluid	<input type="checkbox"/>	[fluid] [m3]
Electrical Safety	Electrical equipment and installations	<input type="checkbox"/>	[voltage] [V], [current] [A]
	High Voltage equipment	<input type="checkbox"/>	[voltage] [V]
Chemical Safety	CMR (carcinogens, mutagens and toxic to reproduction)	<input type="checkbox"/>	[fluid], [quantity]
	Toxic/Irritant	<input type="checkbox"/>	[fluid], [quantity]
	Corrosive	<input type="checkbox"/>	[fluid], [quantity]
	Oxidizing	<input type="checkbox"/>	[fluid], [quantity]

	Flammable/Potentially explosive atmospheres	<input type="checkbox"/>	[fluid], [quantity]
	Dangerous for the environment	<input type="checkbox"/>	[fluid], [quantity]
Non-ionizing radiation Safety	Laser	<input type="checkbox"/>	[laser], [class]
	UV light	<input type="checkbox"/>	
	Magnetic field	<input type="checkbox"/>	[magnetic field] [T]
Workplace	Excessive noise	<input type="checkbox"/>	
	Working outside normal working hours	<input type="checkbox"/>	
	Working at height (climbing platforms, etc.)	<input type="checkbox"/>	
	Outdoor activities	<input type="checkbox"/>	
Fire Safety	Ignition sources	<input type="checkbox"/>	
	Combustible Materials	<input type="checkbox"/>	
	Hot Work (e.g. welding, grinding)	<input type="checkbox"/>	
Other hazards			